Electronic Supplementary Material (ESI) for Physical Chemistry Chemical Physics.

Supporting Information: Theoretical insight into the formation and stability of reactive oxygen species in cryptochrome

Padmabati Mondal* and Miquel Huix-Rotllant*

Aix Marseille Univ, CNRS, ICR, Marseille, France

E-mail: padmabati.mondal@gmail.com; miquel.huix-rotllant@univ-amu.fr

Phone: +33 (0)484529201. Fax: +33 (0)4912888758

S1: Statistical significance of the results regarding position of oxygen species in cryptochrome

In order to show the statistical significance of the results we obtained in terms whether the oxygen stays or leave the C4a cavity from one trajectory, 5 trajectories with different initial conditions are run for each systems and the C4a-OO1 distances for each of them are recorded. These distances for each cases are shown in Figure 1. It is evident from the figure that for ^{2}[FADH^{+}–$O_2^{\bullet-}$], ^{3}[FADH$^{\bullet-}$–$O_2^{\bullet-}$], ^{2}[FAD$_{ox}$–$HO_2^{\bullet}$], ^{3}[FAD$^{\bullet-}$–$HO_2^{\bullet}$] (H, I, J and K), the oxygen species i.e. the ROS is staying close to the lumiflavin ring due to strong electrostatic interactions for all the 5 trajectories which also verifies the statistical significance of the results obtained from the single trajectory simulations. In system ^{2}[FAD$_{ox}$–O$_2$] (A), i.e. the cryptochrome with fully oxidized FAD, molecular oxygen is partially staying near the C4a cavity (for 3 out of 5 trajectories). On the other hand, for cryptochrome with ^{4}[FADH$^{\bullet}$–O$_2$] (C), the triplet oxygen species goes farther away from the C4a cavity. Therefore, it is statistically verified that only the doublet oxygen species i.e. the superoxide and the hydroperoxyl radical are stabilized in the binding pocket close to the N5(H) of FAD species as well as to the Cys416 and Trp420 of cryptochrome.

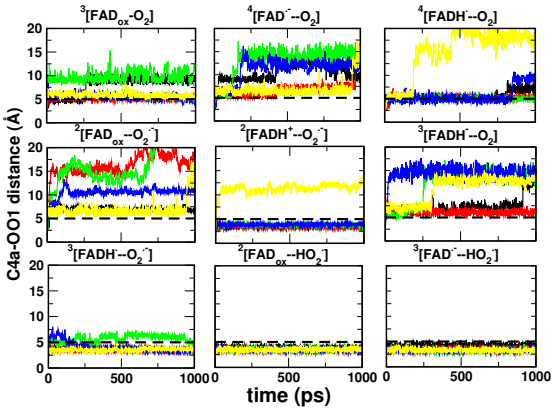

Figure 1: C4a-OO1 distance for 5 trajectories with different initial conditions for each of the nine systems (**A** to **K**). The horizontal black dashed line defines the radius of the C4a cavity.

S2: Geometrical parameters for lumiflavin in five different redox states

For comparison of the bond, angle and dihedrals, the gas phase QM-optimized geomtries for five different redox states of lumiflavin are shown in Figure 2.

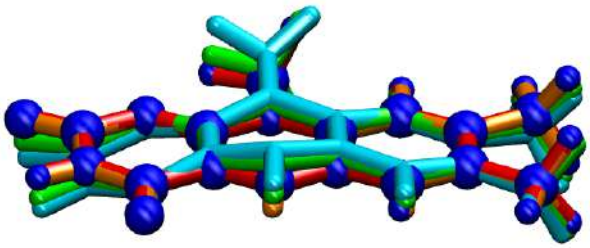

Figure 2: Optimized structures at the B3LYP/def2-TZVPP level in the gas phase. FAD_{ox} (blue CPK), $FAD^{\bullet}$ (red), $FADH^{\bullet}$ (orange), $FADH^{-}$ (green), $FADH_2$ (cyan).

Moreover, individual bonds, angles and dihedrals for all five redox states of lumiflavin are given below in Z-matrix representation. A closer inspection to the individual bond length, angle and dihedrals, we observe the main variations between the 5 redox forms in the atoms forming the diimine bond (N5=C4a-C10a=N1), which accept two electrons and two protons. Indeed, we found variations of 0.1 on average for the N5=C4a bond length, C4a-C10a and C10a=N1 bonds when the chromophore is reduced, while the other bond lengths are essentially invariant (0.02 differences on average with respect to FADox). These 6 angles corresponding to the diimine bond varies about 10 degree with respect to the fully oxidized form, while the variation for the rest of the angles remain within +/-2 degrees. For the dihedrals-the maximum variation of dihedrals is 25 degree (only 2 dihedrals corresponding to diimine bond) and for the rest dihedrals, the variation is within 5 degree.

```
c
n     1 nc2
c     2 cn3          1 cnc3
```

```
n     3 nc4          2 ncn4          1 dih4
c     4 cn5          3 cnc5          2 dih5
c     5 cc6          4 ccn6          3 dih6
n     1 nc7          6 ncc7          5 dih7
c     7 cn8          1 cnc8          6 dih8
c     8 cc9          7 ccn9          1 dih9
n     9 nc10         8 ncc10         7 dih10
c     8 cc11         9 ccc11        10 dih11
c    11 cc12         8 ccc12         9 dih12
c    12 cc13        11 ccc13         8 dih13
c    13 cc14        12 ccc14        11 dih14
o     3 oc15         2 ocn15         1 dih15
o     5 oc16         4 ocn16         3 dih16
c    13 cc17        14 ccc17         9 dih17
c    12 cc18        13 ccc18        14 dih18
c     7 cn19         8 cnc19         9 dih19
h     4 hn20         3 hnc20         2 dih20
h    17 hc21        13 hcc21        14 dih21
h    17 hc22        13 hcc22        14 dih22
h    17 hc23        13 hcc23        14 dih23
h    18 hc24        12 hcc24        13 dih24
h    18 hc25        12 hcc25        13 dih25
h    18 hc26        12 hcc26        13 dih26
h    11 hc27        12 hcc27        13 dih27
h    14 hc28         9 hcc28        10 dih28
h    19 hc29         7 hcn29         8 dih29
h    19 hc30         7 hcn30         8 dih30
```

h	19 hc31	7 hcn31	8 dih31	
h	10 hn32	5 hnc32	4 dih32	
h	1 hn33	2 hnc33	15 dih33	

	FAD_{ox}	$FAD^{\bullet -}$	$FADH^{\bullet}$	$FADH^{-}$	$FADH_2$
nc2	1.300624	1.319699	1.356284	1.418305	1.389537
cn3	1.377110	1.389754	1.414709	1.381378	1.373446
cnc3	120.032	121.403	121.646	121.051	113.435
nc4	1.410638	1.414832	1.389381	1.414390	1.406847
ncn4	117.729	116.630	117.088	117.369	127.286
dih4	0.013	4.061	0.063	2.885	-1.600
cn5	1.375245	1.386609	1.399607	1.406292	1.431177
cnc5	127.698	127.618	121.147	119.552	114.273
dih5	-0.006	-9.852	-0.035	16.440	2.922
cc6	1.498659	1.503538	1.410829	1.418674	1.359478
ccn6	112.626	112.584	120.107	119.404	120.956
dih6	0.004	7.951	0.022	-17.392	-2.770
nc7	1.378807	1.395981	1.308622	1.331612	1.378746
ncc7	115.753	116.484	123.468	125.326	120.440
dih7	-179.975	175.567	-179.971	-176.734	-178.268
cn8	1.383194	1.403602	1.374237	1.359908	1.429977
cnc8	120.964	119.910	119.863	118.620	116.477
dih8	-0.060	6.309	-0.005	-0.157	23.506
cc9	1.412974	1.422496	1.416127	1.404298	1.404365
ccn9	118.580	118.808	117.600	116.946	118.364
dih9	0.056	-3.946	-0.029	-1.473	-24.478

nc10	1.363941	1.367826	1.371842	1.391527	1.398088
ncc10	121.654	121.349	126.242	126.625	118.513
dih10	-0.016	0.612	0.048	1.628	-0.536
cc11	1.399815	1.415621	1.395618	1.390783	1.386250
ccc11	118.674	117.761	117.566	118.107	119.248
dih11	179.982	178.735	179.976	177.439	179.125
cc12	1.387446	1.393778	1.392976	1.405425	1.400028
ccc12	121.285	121.562	122.296	122.855	121.987
dih12	0.011	1.282	0.003	-0.860	-1.903
cc13	1.418771	1.427894	1.408468	1.393166	1.397972
ccc13	120.239	120.610	119.578	118.775	118.766
dih13	-0.002	-0.614	0.002	1.090	1.287
cc14	1.378443	1.382041	1.386770	1.399593	1.397043
ccc14	118.387	118.057	118.571	118.827	119.030
dih14	-0.005	-0.318	-0.007	-0.126	0.312
oc15	1.211144	1.230692	1.213839	1.233657	1.214087
ocn15	123.405	123.553	123.862	124.541	124.530
dih15	-179.997	-176.493	179.986	178.935	178.018
oc16	1.209619	1.230260	1.227909	1.245987	1.223411
ocn16	123.050	123.156	124.454	121.583	120.830
dih16	-179.992	-173.595	179.976	179.783	-178.161
cc17	1.504522	1.507827	1.504388	1.507651	1.505707
ccc17	120.619	120.916	120.203	119.788	119.804
dih17	-179.999	-179.704	-179.995	179.115	178.957
cc18	1.503075	1.506476	1.504549	1.507639	1.506132
ccc18	120.305	120.152	120.783	121.532	121.386
dih18	179.996	178.468	179.997	-179.885	-179.554

cn19	1.464407	1.470000	1.458513	1.444828	1.447932
cnc19	119.937	119.827	119.696	119.248	120.196
dih19	-179.958	-161.371	-179.969	178.277	168.352
hn20	1.010583	1.014017	1.009579	1.007339	1.009210
hnc20	115.494	115.213	115.975	116.413	116.203
dih20	179.999	-179.551	-179.982	-179.181	0.205
hc21	1.088262	1.093222	1.088691	1.090212	1.088899
hcc21	110.853	110.798	111.154	110.963	111.181
dih21	-0.016	0.065	-0.001	0.040	-0.110
hc22	1.092369	1.097952	1.092383	1.094386	1.092700
hcc22	111.622	111.745	111.538	111.970	111.602
dih22	120.249	120.372	120.357	120.253	120.255
hc23	1.092361	1.097721	1.092377	1.094460	1.092757
hcc23	111.625	111.729	111.539	111.958	111.576
dih23	-120.281	-120.213	-120.360	-120.168	-120.458
hc24	1.092295	1.097817	1.092549	1.094957	1.092849
hcc24	111.247	111.567	111.523	112.212	111.771
dih24	59.339	60.290	59.535	59.507	59.038
hc25	1.092294	1.097171	1.092558	1.095112	1.093069
hcc25	111.247	111.185	111.519	112.237	111.786
dih25	-59.366	-58.783	-59.639	-60.347	-60.464
hc26	1.088255	1.092402	1.088587	1.090458	1.089409
hcc26	111.429	111.250	111.236	110.854	111.143
dih26	179.986	-178.952	179.950	179.578	179.296
hc27	1.079043	1.078100	1.078887	1.080324	1.080934
hcc27	118.584	118.948	118.310	118.047	118.285
dih27	179.988	176.032	-179.996	-179.297	-178.990

hc28	1.081784	1.085901	1.083350	1.084723	1.083603
hcc28	116.785	116.602	118.429	118.065	118.462
dih28	0.008	0.159	179.999	-179.699	179.753
hc29	1.089405	1.070000	1.090859	1.098003	1.096523
hcn29	109.909	109.471	110.338	112.096	113.297
dih29	60.037	84.386	60.294	61.428	78.417
hc30	1.082765	1.070000	1.083374	1.084519	1.088588
hcn30	107.856	109.471	107.757	107.723	109.973
dih30	179.821	-155.614	179.980	-179.438	-159.192
hc31	1.089462	1.070001	1.090899	1.093762	1.088331
hcn31	109.927	109.471	110.344	110.269	109.023
dih31	-60.414	-35.614	-60.351	-59.049	-42.061
hn32			1.012707	1.008760	1.009687
hnc32			116.030	113.177	112.768
dih32			0.113	13.848	13.424
hn33					1.005298
hnc33					114.379
dih33					-4.943

S3:Effect of electrostatic force field models on the dynamics of FAD-O_2 system

To validate our results using mulliken charges, we have performed MD dynamics for the ^{3}[FADH$^\bullet$- $O_2^{\bullet-}$] system using Merz-Kollmann (MK) type ESP fitted charges and compared them with the reported results (see Figure 3). The C4a-OO1 distances, which indicate the strength of hydrogen bonding between FAD and oxygen, are quite similar (below-left panel). Furthermore, the binding location of the superoxide with MK-ESP-fitted charges

(below-right panel) is the same as with the Mulliken charge (main text Figure 4 lower left panel).

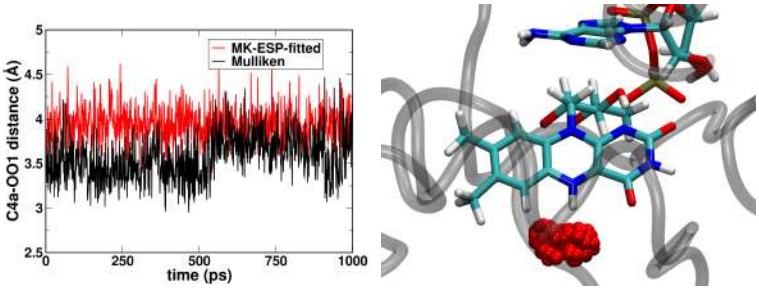

Figure 3: Effect of electrostatic force fields on the dynamics of FAD-O_2 complex. Left : Evolution of C4a-OO1 distance, right : binding position of oxygen species in the pocket.